Kinetic Study of Seawater Reverse Osmosis Membrane Fouling

ARTICLE *in* ENVIRONMENTAL SCIENCE & TECHNOLOGY · SEPTEMBER 2013

Impact Factor: 5.33 · DOI: 10.1021/es402138e · Source: PubMed

Environmental Science & Technology

Article

pubs.acs.org/est

Kinetic Study of Seawater Reverse Osmosis Membrane Fouling

Muhammad Tariq Khan,[†] Carmem-Lara de O. Manes,[†,‡] Cyril Aubry,[†] Leonardo Gutierrez,[§] and Jean Philippe Croue*[,†]

[†]Water Desalination and Reuse Center, King Abdullah University of Science and Technology (KAUST), Thuwal, Saudi-Arabia

[‡]Vale Institute of Technology (ITV), Rua Boaventura da Silva 955, Belem, Para, Brazil

[§]Department of Civil and Environmental Engineering, Center of Advanced Materials for the Purification of Water with Systems, University of Illinois at Urbana−ChampaignUrbana, Illinois 61801, United States

Supporting Information

ABSTRACT: Reverse osmosis (RO) membrane fouling is not a static state but a dynamic phenomenon. The investigation of fouling kinetics and dynamics of change in the composition of the foulant mass is essential to elucidate the mechanism of fouling and foulant−foulant interactions. The aim of this work was to study at a lab scale the fouling process with an emphasis on the changes in the relative composition of foulant material as a function of operating time. Fouled membrane samples were collected at 8 h, and 1, 2, and 4 weeks on a lab-scale RO unit operated in recirculation mode. Foulant characterization was performed by CLSM, AFM, ATR-FTIR, pyrolysis GC-MS, and ICP-MS techniques. Moreover, measurement of active biomass and analysis of microbial diversity were performed by ATP analysis and DNA extraction, followed by pyro-sequencing, respectively. A progressive increase in the abundance of almost all the foulant species was observed, but their relative proportion changed over the age of the fouling layer. Microbial population in all the membrane samples was dominated by specific groups/species belonging to *Proteobacteria* and *Actinobacteria* phyla; however, similar to abiotic foulant, their relative abundance also changed with the biofilm age.

1. INTRODUCTION

Seawater reverse osmosis (SWRO) process has played an essential role in producing fresh water for human consumption.[1,2] To improve this water treatment technique, a substantial amount of research has been conducted, i.e., development of new membranes and pretreatment strategies to benefit capital and operational costs.[3,4] Regardless of all the available state of the art technologies, fouling of desalination membranes remains as a problem which seriously impacts the performance and economic viability of this water treatment operation.[3,5,6]

Membrane fouling is a complex and dynamic phenomenon as different phases are involved in the progressive development of a fouling layer. During organic, inorganic, and colloidal fouling the involved steps include foulant−membrane interactions (rapid initial step) and foulant−foulant interactions (gradual long-term step).[7] Similarly, different steps can be distinguished for microbiological fouling, i.e., conditioning film formation by glycoproteins and/or other organics,[8−10] cell attachment, cell growth, and cell dispersion.[11−13] Different phases taking place in the development of a fouling layer (i.e., kinetic aspect) can be tracked down through monitoring the changes in relative abundance and diversity of the fouling species over time. All previous fouling characterization studies were conducted using synthetic water as feedwater and/or focused on characterization of autopsied modules representing only a transitory state of a prevailing fouling scenario. Recently, Monruedee et al.[14] analyzed the changes in morphology and elemental composition of a SWRO membrane fouling layer through periodic samplings, i.e., 2−20 h. However, this system was fed with a synthetic solution and only ultrastructural fouling characterization techniques were used. Another kinetic fouling study (operation time 8 h to 24 days) was carried out by Ivnitsky et al.[15] with nanofiltration (NF) membranes used to treat wastewater.

Biofouling is considered the main drawback of SWRO membranes, affecting approximately 70% of the seawater RO membrane systems.[16] Although biofilm formation phenomenon has been extensively investigated, a significant fraction of these studies have focused on systems rather than SWRO membranes. Moreover, there are only a few studies in the literature on microbial diversity or chemical composition of SWRO membrane biofilms, and no comprehensive study on the changes in microbial community and chemical composition of the biofilm matrix with operating time. Briefly, Manes et al.[17] studied changes in the profile of microbial diversity of full-scale SWRO membranes biofilm with operating times ranging from 10 to 330 days. *Betaproteobacteria* affiliated with the genus *Ideonella* were identified as potential primary colonizers. In the case of relatively mature biofilm, the majority of bacterial population belonged to phyla *Alphaproteobacteria* or *Planctomycetes*. However, since the membranes were subjected to chemical cleaning procedures, the biofouling profiles might

Received: May 14, 2013
Revised: August 11, 2013
Accepted: August 28, 2013
Published: August 29, 2013

have been impacted. Horsch et al.[18] reported *Gammaproteobacteria* and *Betaproteobacteria* as the major groups in early stage and relatively mature form, respectively, of NF membrane biofilm fed by ultrafiltration (UF) pretreated water from an oligotrophic reservoir. Zhang et al.[1] identified *Gammaproteobacteria and Alphaproteobacteria* as 30% and 61.2% of the total microbial community, respectively, in the biofilm of SWRO membranes. Dominance of *Alphaproteobacteria* over other bacterial communities in the fouling layer of full-scale SWRO membranes, fed by Red Sea water, has also been observed in our recently published study.[19]

The objectives of this SWRO membrane biofouling kinetics and dynamics study, conducted at lab scale, were to find (a) initial colonizing bacteria, (b) changes taking place in the bacterial population from initial stage to relatively mature biofilm stage, and (c) changes in chemical composition of the biofilm matrix over the age of biofilm and their possible correlation with the microbial community profile. Fouled membranes operated from 8 h to 4 weeks were subjected to various characterization techniques including fouling load analysis, adenosine-5′-triphosphate (ATP) analysis, atomic force microscopy (AFM) analysis, confocal laser scanning microscopy (CLSM) analysis, attenuated total reflection (ATR)/potassium bromide (KBr) pellet–Fourier transform infrared spectroscopy (FTIR) analysis, pyrolysis gas chromatography–mass spectrometry (Pyro/GS-MS) analysis, inductively coupled plasma optical emission spectroscopy (ICP-OES) elemental analysis, and phylogenetic analysis. In addition to the fouling layer characterization, feedwater quality was also analyzed to assess its fouling potential.

2. MATERIALS AND METHODS

2.1. Description of SWRO Lab-Scale Plant. The design and setup of the SWRO lab-scale plant are shown and described in the Supporting Information (SI). The unit consisted of three flat membrane cells in series with a membrane coupon active surface area and feed spacer thickness of 78 cm^2 and 44 mil, respectively, operating in recirculation mode (SI Figure S1). Red Sea water prefiltered through a 10-μm cartridge filter (Polygard-CR, Millipore, USA) was used as feedwater and was renewed every 48 h. The operating pressure was kept constant at 60 bar with a cross-flow velocity of 0.091 m/s. SW30-HR membranes from DOW Filmtec were used. Four sets of experiments were conducted at 8 h and 1, 2, and 4 weeks of operation from April 21 until June 28, 2011.

The lab-scale unit was carefully cleaned and disinfected between each run following the protocol described in SI. After thorough cleaning, virgin membrane coupons were installed. Prior to experiments with seawater, coupons were compacted by operating with autoclaved deionized (DI) water at 30 bar feed pressure for 48 h. Fouled membrane coupons were subjected to fouling characterization. Fouling of 8 h membranes was characterized only by FTIR, AFM, and CLSM analyses because of insufficient amount of deposited foulant.

2.2. Seawater Characterization. The feedwater (FW) quality was characterized by silt density index (SDI_5), total/dissolved organic carbon (TOC/DOC; TOC-V_{CPH} Analyzer, Shimadzu, Japan), adenosine-5′-triphosphate (ATP; ATP Analyzer, Celsis, USA), heterotrophic plate count (HPC), and flow cytometric (FCM; Accuri C6 Flow Cytometer, USA) analyses. Additionally, elemental analysis was performed by ICP-OES (Varian, USA).

SDI_5 was determined according to the ASTM D4189-07 method.[20] Heterotrophic plate count was conducted by following Reasoner and Geldreich's method,[21] using marine agar as a nutrient medium to grow and enumerate heterotrophic bacteria. Total cell count was determined by the FCM method adapted from Nocker et al.[22] Cells in water samples were stained with a cell membrane permeable nucleic acid fluorescent probe (SYBR Green I, concentration 1×, incubation time 15–20 min) followed by flow cytometric analysis. ATP concentration, an indicator of active biomass in water samples, was determined by the luciferin–luciferase bioluminescence reaction method.[23] Interference by salts in the ATP measurement of seawater was minimized by diluting the sample 50 times with sterile Tris-HCl Buffer at a pH 7.4.[24] With the exception of elemental analysis, all the measurements were carried out in triplicate and once a week. Additionally, marine humic-like material was isolated from 100 L of Red Sea water using the comprehensive XAD-8/XAD-4 resins extraction protocol proposed by Leenheer et al.[25]

2.3. Chemical and Ultrastructural Analysis of Fouling Layer. Fouling load measurement was carried out by weighing dried fouled and virgin membranes of the same surface area in triplicate. The difference between these two weight values was considered as fouling mass deposited on the membrane surface.

Elemental analysis with ICP-OES was performed after digestion of foulant layer with trace element analysis grade nitric acid (HNO_3, Trace SELECT Ultra, Sigma-Aldrich). Foulant material digestion involved the treatment of 2–5 cm^2 piece of fouled membrane with 1 mL of HNO_3 in a Pyrex glass tube kept at 100 °C for 1 h. After completion of digestion, the sample was diluted with ultrapure water (resistivity 18 MΩ-cm, Milli-Q, Millipore, Barnstead, USA) to a final volume of 10 mL.

Other direct and indirect fouling characterization procedures used in this study include ATP contents and infrared (IR) spectroscopic analyses of fouled membranes, and pyrolysis/GC-MS analysis of isolated foulant material. Details of these protocols have been described in our recently published work.[19]

2.3.1. Confocal Laser Scanning Microscopic (CLSM) Analysis. Staining protocol was adapted from Chen et al.[26,27] The stains used in this investigation included SYBR Green I (SG) to stain cells (ex/em 497/520, concentration 1×, incubation time 30 min), SYPRO Orange to stain proteins (ex/em 470/570, concentration 5×, incubation time 30 min), and Concanavalin A (Con A) to target polysaccharides (ex/em 495/519, concentration 200 μg/L, incubation time 30 min), and were purchased from Invitrogen, USA. An approximately 1-cm^2 piece of fouled membrane, initially fixed with 2% paraformaldehyde and kept at −20 °C to preserve the specimen until analysis, was rinsed with 10 mM phosphate buffer saline (PBS, pH 7.4). Staining was carried out in dark brown microtubes by incubating the sample with the dyes at room temperature. During incubation, microtubes were placed on a horizontal orbital shaker (IKA, Germany) operating at 80 rpm. A half milliliter of each staining agent solution was used. After every staining step the samples were rinsed with 10 mM PBS buffer.

Imaging was carried out with a LSM710 laser scanning confocal microscope (Zeiss, Germany) using a 40× lens and ZEN2009 software. SG and Con A were analyzed in a common channel since both have emissions in the same region. However, the difference in the fluorescence intensities of these two probes (relatively higher fluorescence intensity for SG) was used to distinguish them from each other.

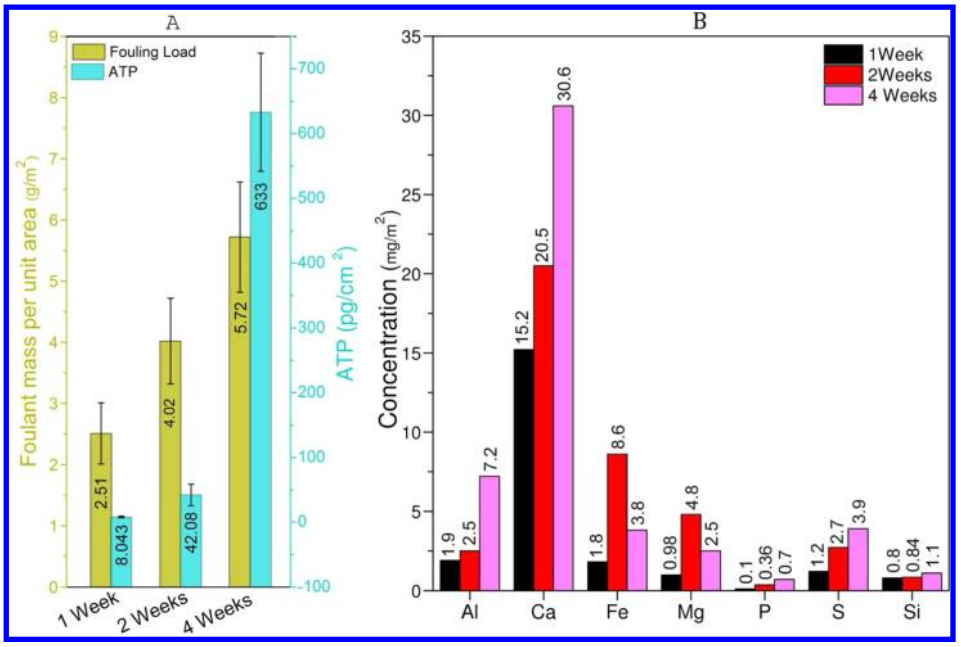

Figure 1. (A) Fouling load, ATP, and (B) ICP-OES analyses of fouled membranes showing increase in both active biomass and overall foulant mass accumulated on the membranes with increasing operating time. The concentration per unit surface area of the majority of multivalent cations increased with operating time. Error bars correspond to standard deviation values.

2.3.2. Atomic Force Microscopy (AFM) Analysis. Preparation of electrolyte solutions and AFM probes is described in the SI. AFM imaging of virgin and fouled membranes were conducted in 1 Mm NaCl solution in intermittent mode. The membrane surface was scanned with the colloidal probe while recording topography and phase signals simultaneously. The phase signal value was set to zero when the probe was located at a significant distance from the surface (≥20 μm). The recorded data were processed with PicoImage Basic software (Agilent, USA) to overlay phase and topography signals. Force versus distance curves between the colloidal probe and virgin or fouled membrane were conducted in contact mode. The spring constant of the cantilever were measured following the thermal tuning method developed by Hutter and Bechhoefer[28] and using the Thermal K module (Agilent, USA). Force curves were acquired at a 0.4 μm/s rate and starting at a distance of 3 μm from the surface of the membrane. Multiple force curves were recorded for every ionic strength tested at different locations of the membrane surface. The approaching force profiles were analyzed following Li and Logan[29] methodology. Briefly, gradient force (i.e., defined as the slope of the 5 data points surrounding the point where the gradient is calculated) was calculated on the approach part of the adhesion curve force, and 4 different regions were delineated (SI Figure S2): noninteraction region (slope equal to zero), noncontact region, contact region, and constant compliance (constant negative slope). Distinction between noncontact and contact phase regions was obtained with the change of the slope of the gradient force curve. For some force curves this distinction was facilitated by the presence of a transition region easily detectable on the gradient force curve. However, for other curves this transition region was not present and distinction between noncontact and contact phase length was not clear. Adhesion energies (i.e., energy required to detach the probe from the surface) were calculated from the retraction force profiles by integrating the pull-off forces by the separation distance using the trapezoidal rule.[30]

2.4. Bacterial Community Composition Analysis. Membrane and water samples were subjected to nucleic acid extraction and next generation sequencing following the protocols described by Khan et al.[19]

3. RESULTS AND DISCUSSION

3.1. Feed Water Characteristics. The quality and especially the diversity of microbial population of the Red Sea along the coast of Saudi Arabia are not very well documented. Therefore, it was essential to observe the temporal variations in the profile of feedwater quality in order to monitor possible environmental changes that might affect biofilm development. Bio- and physicochemical quality indicators of intake water were monitored during the period experiments were conducted. SDI_5, turbidity, TOC/DOC, elemental analysis, cell counts, ATP, and the microbial community diversity results are summarized in SI Figure S3 and Table S1and S2.

No significant change could be observed in the monitored water quality parameters. The average quality of RO feedwater after 10-μm cartridge prefiltration, was as follows: SDI_5 ≤5; TOC 0.98 mg/L; ATP concentration 55 ng/L; HPC approximately 10^4 cfu/mL; total cell count 2.8×10^3 cell/μL. The 10-μm prefiltration improved the SDI_5 value of the Red Sea water while the other parameters were not affected.

Besides the above-mentioned parameters, a 3-month temporal survey of intake water microbial community was also performed by pyro-sequencing analysis of the 16S rRNA gene and the taxonomic classification and affiliation of sequences. The distribution and relative abundance of the major phyla from the water samples are shown in SI Figure S3B. All samples were mainly represented by *Cyanobacteria* (pico-phytoplankton) and *Proteobacteria* phyla followed by *Bacteroidetes* with variable abundances along the sampling period. Whereas in all samples *Alphaproteobacteria* class (*Proteobacteria*) affiliated sequences were dominant (reaching up to 55% of the sequences in one sample (Feed_5)), the

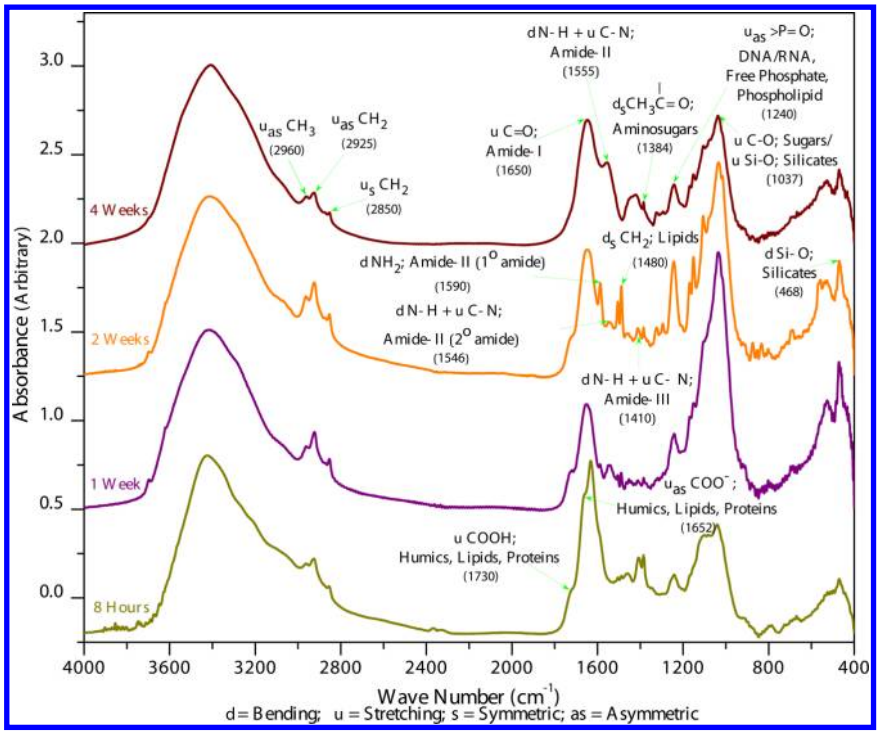

Figure 2. FTIR spectra of foulant materials of RO membranes running for 8 h, 1 week, 2 weeks, and 4 weeks.

Synechococcus genera was considerably the most abundant phylotype among the *Cyanobacteria* phyla with 54% of sequences at Feed_2 (SI Table S1). However, the distribution of major phylotypes (≥3%) revealed no drastic changes in microbial community composition between samples at approximately 3-month intervals. Dominant groups were always dominant, indicating that intake water presented a relatively stable microbial distribution. Dominance of *Cyanobacteria* in the photic zone of Red Sea has also been reported by Qian et al.[31] in their study conducted at off-shore locations associated with deep sea brine pools.

3.2. Changes in Fouling Profile with Increasing Operation Time. Fouling load analysis was conducted to determine the level and rate of fouling layer development. The fouling load of the membrane nearly doubled from 1 week operation (2.51 ± 0.47 g/m^2) to 2 weeks operation (4.02 ± 0.66 g/m^2). After 4 weeks, the fouling load was further increased (5.72 ± 0.85 g/m^2) (Figure 1A). This observation confirms that there was a dynamic process of foulant deposition/accumulation on the membrane surface. The ATP content followed the same trend and it was observed that higher the fouling load, the higher the ATP content. This result confirmed a biofilm development with operating time and showed its importance in the overall fouling process. As the fouling layer was developed with operating time, membrane permeability was observed to decrease (SI Figure S4). Major inorganic elements accumulated in the fouling layer were analyzed with ICP-OES. Data showed that the concentration of multivalent cations (i.e., Al and Ca) and nonmetallic elements (i.e., P and S) gradually increased with operation time (Figure 1B). Fe and Mg concentrations increased from 1.8 to 8.6 mg/m^2 and from 1.0 to 4.8 mg/m^2 from the first to the second week, respectively, but then declined to 3.8 and 2.5 mg/m^2 at the fourth week, respectively. Inorganic elements, especially multivalent cations, are known to play a vital role in biofouling[32,33] and organic fouling[14,34] due to their strong tendency to form complexes with negatively charged moieties. As shown later in this investigation, the relatively higher abundance of complexing cations (e.g., Fe and Mg) in the initial fouling layer than in comparatively mature fouling layer agreed with the existence of more negatively charged sites at the early stage of the fouling process resulting in higher uptake of cations.

ATR-FTIR difference spectra showed progressive development of fouling layer. However, due to overlapping with membrane material signals and low intensities, signals of foulant material were not well resolved and were difficult to interpret (SI Figure S5). KBr pellet IR spectra of foulant material, isolated from membranes, had comparatively better resolved bands (Figure 2). Interestingly, IR spectrum of 8-h sample was similar to that of marine hydrophilic acid plus neutral organics, published by Leenheer,[35] showing a strong band of carboxyl/carboxylate group overlapped with amide-I band. In addition, amide-II peak, a characteristic IR signal of proteins and aminosugars typically found near 1550 cm^{-1}, was not detected. From this profile, Leenheer suggested that amides were most probably lactams of five- to seven-membered rings where the amide-II band does not exist.[35] Progressive evolution of amide bands, characteristic functional groups of proteins, i.e., amide I (mainly C═O stretching vibration at 1650 cm^{-1}), amide-II (out of phase combination of N−H bending and the C−N stretching vibration at 1555 cm^{-1}), and amide-III (in phase combination of N−H bending and the C−N stretching vibration 1410 cm^{-1}),[36] were observed from 8-h to 4-weeks samples. Similar to proteins, the aminosugars (i.e., indicators of bacterial cell wall residues) signal represented by the symmetric bending of CH_3 of *N*-acetyl group at 1384 cm^{-1} [35,37,38] was also found to progressively increase with operating time. The band at 1240 cm^{-1}, detected in all samples, is attributable to either free phosphate and/or phosphodiester backbone of the nucleic acid, i.e., DNA/RNA (PO^{2-} asymmetric stretching). Relative intensity of band at 1037 cm^{-1}, likely a joint sugars and silicates

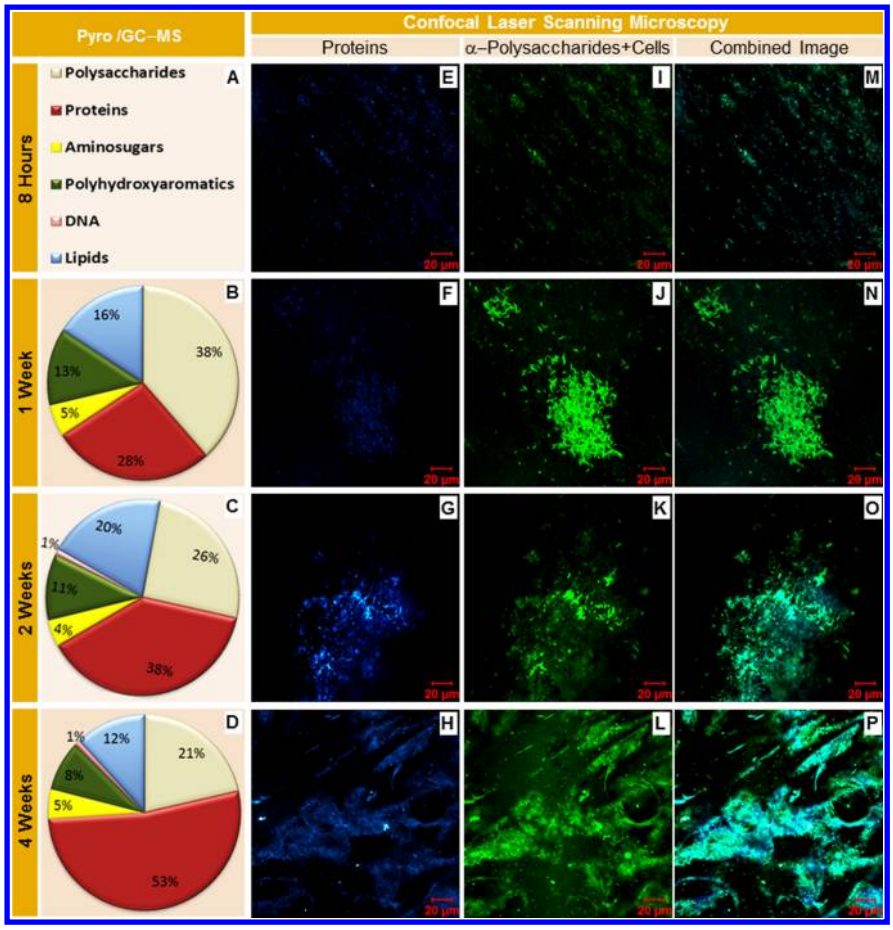

Figure 3. Direct and indirect characterization of the organic composition and morphology of biofilm present on the surface of 8-h to 4-weeks membrane samples. A–D: Biopolymer distribution calculated from pyrochromatograms; CLSM images showing E–H proteins (blue signal from SYPRO Orange), I–L polysaccharide (green signal from Alexafluor 488), and cells (relatively high intensity green signal from SYBR Green I); M–P combined image with all the signals superimposed.

(stretching of C–O and Si–O, respectively)[37,39] band, was considerably increased from 8-h to 1-week sample. This result suggests the accumulation of sugars and/or silicates in the fouling layer of 1 week age. After 1 week, due to increase in proteins, the relative intensity of this band was gradually decreased. The relative intensity of alkyl group (CH_3 asymmetric stretching at 2960 cm^{-1}; CH_2 asymmetric and symmetric stretching at 2925 and 2850 cm^{-1}, respectively) and carboxyl group signals, likely coming from lipids, increased from 8 h to 2 weeks. This finding can be explained by initial bacterial growth resulting in increased lipid concentration in the fouling layer. After 4 weeks, the relative intensity of these signals decreased probably because of the release of extracellular polymeric substances (EPS) containing mainly sugars/proteins.

3.3. Major Organic Constituents of SWRO Membrane Biofilm. Pyro/GC-MS, a semiquantitative analysis approach, was used to make a comparative analysis of organic composition of membrane foulant samples. The relative proportion of a biopolymer was calculated as the area of its signature pyro-fragment peaks divided by the total peak area of the pyro-chromatogram. The target of this analysis was to observe the evolutionary trend of different biopolymers while understanding that the calculated distribution profile for a specific sample may not reflect its exact composition because different biopolymers exert different pyrolysis yield.[40] The detection of prominent signals of DNA (furanmethanol pyro-fragment) and aminosugars (acetamide pyro-fragment) in the foulant samples of 1- to 4-weeks membranes, considered as the signposts of living or recently died microorganisms, was an evidence of biofouling/microbial activity occurring on all the membranes. However, the profile of biopolymer signals in the pyrochromatograms (SI Figure S7) and their calculated relative abundance (Figure 3A–D) changed with operating time, therefore revealing changing patterns of fouling layer composition. These changes could be related to the dynamic stages involved in the biofilm formation over time. Proteins detected in all the samples were composed of phenylalanine (toluene, styrene as pyrolysis byproducts), tyrosine (phenol, p-cresol as pyrolysis byproducts), and tryptophan (indole, methyl indole as pyrolysis byproducts) aminoacids.[41] A significant increase in the relative proportion of proteins (associated with the decrease in relative abundance of polysaccharides) was observed from 1-week (i.e., 28%) to 4-weeks (i.e., 53%) membrane coupons. This observation is evident from the continuous increase in relative abundance of styrene peak (2.80, 5.25, and 12.74% area for 1-week, 2-weeks, and 4-weeks samples, respectively), and continuous decrease in the phenol/p-cresol peak ratio (1.64, 1.18, and 1.08 for 1-week, 2-weeks, and 4-weeks samples, respectively).[40] Because usually polysaccharides, not proteins, are known to represent the most abundant component of marine microbial EPS,[42] this increase

in relative abundance of proteins after the first week is most likely due to bacterial cellular growth and biofilm maturation (cell decay) resulting in the release of protein-enriched cellular material.[43] Previously, we have observed higher relative abundance of protein characteristic pyro-fragments (i.e., approximately 50%) in the material recovered from full-scale plant SWRO membranes having recent and mature biofilm.[19] Significantly high relative abundance of fatty acids (i.e., C-16) signals in 1-, 2-, and 4-weeks membrane sample (i.e., 16%, 20%, and 12%, respectively) also provides evidence of the presence of material originated from microbial cells.

Another significant difference is the decrease in relative abundance of polyhydroxyaromatics (PHA) from 1-week (13%) to 4-weeks (8%) old membrane foulant samples. The humic-like substance character of the 1-week membrane deposit was clearly indicated by a phenol/p-cresol peak area/height ratio higher than 1 (i.e., 1.64).[40] Interestingly, benzoic acid was detected only in the pyrochromatogram of 1-week membrane foulant (SI Figure S7). Benzoic acid might have different origins. It is known as a pyro-fragment from humic material containing benzene carboxylic structural units.[44,45] Benzoic acid might have also come from phthalates-based plasticizer, used in numerous plastic materials. Kusch[46] reported that the pyrolysis of di-2-ethylhexyl phthalate (DEHP) produces benzoic acid. Phthalates contamination would then have come from the polyvinyl chloride tubing that equipped our cartridge prefiltration setup. To clarify the origin of benzoic acid peak in the 1-week foulant material pyrochromatogram, pyrolysis GC/MS analyses were conducted on the plastic tubing material and on the marine humic material isolated from the Red Sea. As expected, benzoic acid was observed in both pyrochromatograms. In the chromatogram of marine organics (i.e., XAD-4 isolate representing 20% of the Red Sea DOC content) benzoic acid appeared as one of the most abundant peaks, whereas in the pyrochromatogram of tubing material, benzene dicarboxylic acid and ethyl hexanol were the predominant ones (SI Figure S7). However, these compounds were not present in the membrane foulant material. These results support the hypothesis that benzoic acid was derived from marine humic-like substances that preferentially sorbed onto the membrane surface at the early stage of the fouling process. This is in good agreement with the humic-like substance signature highlighted by the phenol/p-cresol peak ratio. In the marine biofilm formation, the important role of humic substances has been reported by Loeb and Neihof.[47] Moreover, Monruedee et al.[14] reported that humics adsorbed quickly onto the SWRO membrane surface.

In addition to the pyro/GC-MS analysis, CLSM was used to explore the chemistry and morphology of intact biofilm. CLSM images showed that the 8-h membrane contained dispersed cells on its surface. Significantly strong signals for polysaccharides and proteins at the locations containing attached cells might be originated from covering of extracellular substances around the cells (Figure 3E, I, M). These signals might also be originated from polysaccharides and proteins present in initially formed film of organics on the surface. On 1-week membrane, it was observed that some selected cells were able to grow and form colonies (Figure 3F, J, N). After 2 weeks there were distinct signals for released EPS (Figure 3G, K, O), and after 4 weeks the biofilm was more mature with a higher accumulation of EPS (i.e., stronger signals for polysaccharides and proteins) and absence of visible bacterial cells (i.e., possibly covered by an EPS layer) (Figure 3H, L, P).

3.4. Interaction Force Measurements Using Atomic Force Microscopy (AFM). *Interaction Forces between Silica Colloidal Probe and Fouled Membrane Surfaces during Approach.* Noncontact and contact lengths of all fouled membrane samples (i.e., 8-h, 1-, 2-, and 4-weeks samples) were 1 order of magnitude larger than those of virgin membrane (i.e., 0 h), suggesting a change of surface characteristics due to accumulation of foulant material (Figure 4A). Topography and phase contrast images confirmed the progressive accumulation

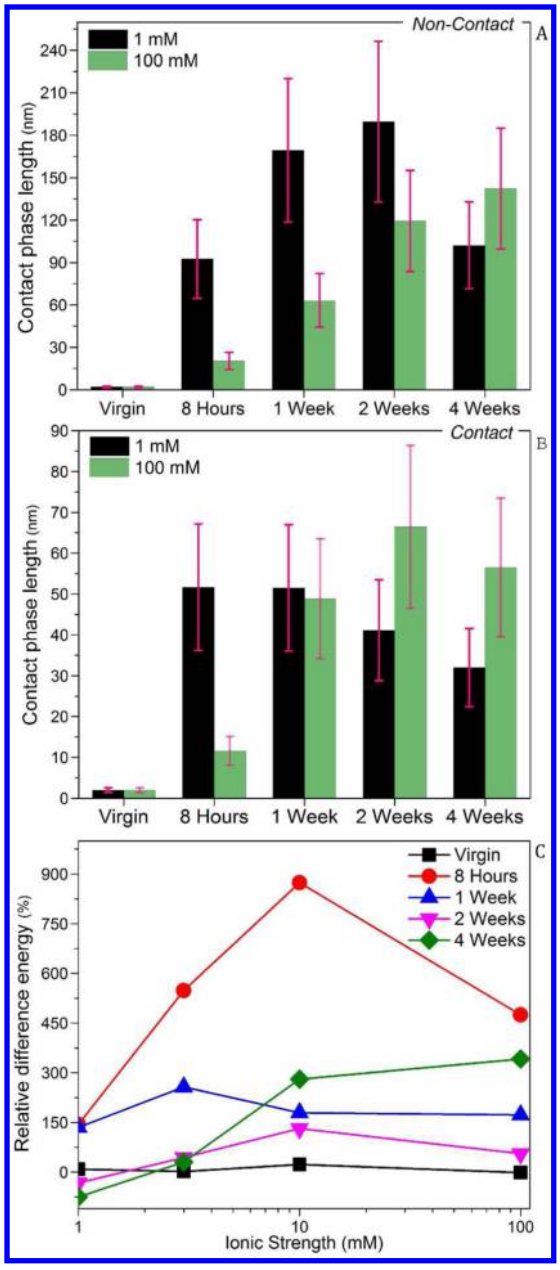

Figure 4. (A) Bar graph of noncontact length for virgin, 8-h, 1-week, 2-weeks, and 4-weeks membrane samples in 1 mM and 100 mM NaCl solutions, (B) bar-graph of contact length for 8-h, 1-week, 2-weeks, and 4-week samples in 1 mM and 100 mM NaCl solutions, and (C) semilog plot of relative difference in adhesion energy between $CaCl_2$ and NaCl solutions of virgin, 8-h, 1-week, 2-weeks, and 4-weeks membrane samples at different ionic strength. Each data point corresponds to the average of 40 measurements. Error bars correspond to standard deviation values.

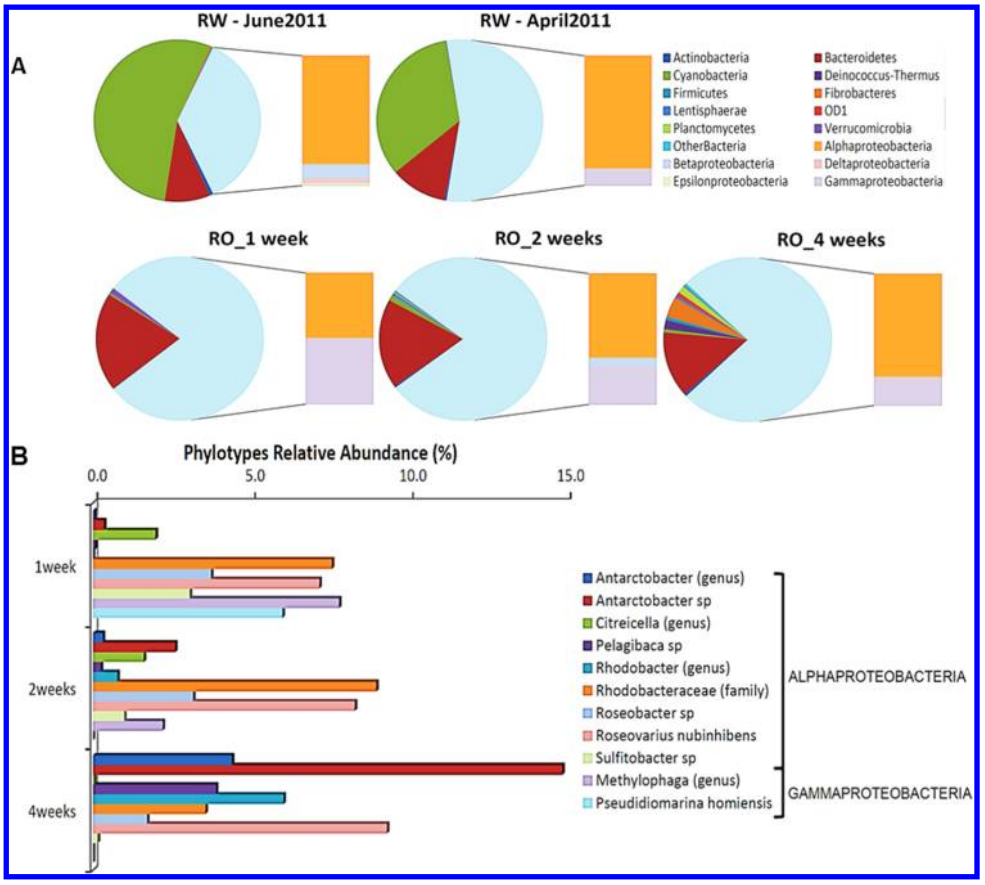

Figure 5. Phylogenetic affiliation and taxonomic distribution of the ribosomal 16S RNA gene sequence data set from lab-scale and full-scale membrane samples. (A) Phyla and *Proteobacteria* class distribution (inset) of sequences. (B) Major taxa (family, genus, and species level) identified in each sample represented >3% of sequences.

of foulant material on the membrane (SI Figure S6). For 8-h, 1-week, and 2-weeks membrane samples, the noncontact length decreased with increasing ionic strength. Nevertheless, these noncontact lengths were significantly larger than those predicted by the theoretical Debye length (10 and 1 nm in 1 mM and 100 mM NaCl solutions, respectively),[48,49] suggesting that in addition to electrostatic effects, steric repulsive forces induced by the presence of polymer-brush-like structures at the membrane surface were also involved.[50] Conformational changes (compression) of the polymer chains with ionic strength would be the cause of the noncontact length decrease for 8-h, 1-week, and 2-weeks membranes. Conversely, noncontact length of 4-weeks membrane sample was lower in 1 mM NaCl solutions compared to 1-week and 2-weeks membrane samples and its magnitude increased with ionic strength. This result suggested that mainly steric interactions were involved during noncontact region and that the foulant adsorbed at the membrane surface was poorly electrostatically charged.

Contact length measured from 1 mM to 100 mM NaCl solutions exhibited a major reduction for 8-h sample, no variation for 1-week sample, and an increase for both 2-weeks and 4-weeks membrane samples (Figure 4B). The significant decrease of contact length with ionic strength observed at 8-h sample clearly indicates a strong compression of the fouling layer due to conformational changes of polymeric chains. Results from FTIR and pyrolysis GC/MS indicates that at this early stage of foulant layer development (8-h), mainly marine-derived humics were deposited on the membrane surface. Humics are mainly identified due to their high content of aromatic and phenolic carbon with carboxyl as main functional groups (i.e., imparting a negative charge at environmentally relevant pH).[49] A previous study reported a considerable charge screening of negatively charged humics and high compression of their polymeric chains with increasing ionic strength[51] (i.e., decreased intermolecular and intramolecular repulsive forces), as similarly observed in 8-h membrane sample.

Conversely, at subsequent stages of fouling layer development (1-, 2-, or 4-weeks samples) an accumulation of nonhumic materials (e.g., polysaccharides and proteins) was detected by FTIR and pyrolysis GC/MS analysis. The increase of contact length recorded for 2-weeks and 4-weeks samples would be the consequence of nonhumics fouling layer compression as similarly observed by Xu and Logan[52] for protein chains. This previous study suggested that protein chains conformation at low ionic strength would lead to very low density layers difficult to detect by stiff cantilevers (i.e., 0.16 nN/nm). However, at high ionic strength, a more compact protein layers were clearly identified.

Interaction Force between Silica Colloidal Probe and Fouled Membrane Surface during Retraction. The relative differences in adhesion energy recorded in $CaCl_2$ and NaCl solutions of similar ionic strength, (i.e., [adhesion energy in $CaCl_2$ − adhesion energy in NaCl]/[adhesion energy in NaCl]) between the silica colloidal probe and the different fouled membrane samples are presented in Figure 4C. The adhesion behavior of the virgin membrane to silica colloid was

not influenced by ionic strength. Foulant deposited on 8-h membrane sample exhibited higher increase in adhesion energy in $CaCl_2$ solution than in NaCl solutions, suggesting Ca^{2+} bridging between the negatively charged silica colloid surface (i.e., SiO^-) and deprotonated carboxyl groups on foulant enriched in humic-like substances (i.e., as detected by FTIR and pyrolysis GC/MS). Previous studies have suggested that calcium ions can form inner-sphere complexes with deprotonated carboxylic groups on NOM molecules while sodium ions can only weakly interact through outer-sphere association.[53] In addition, the stability constant of Ca^{2+} to SiO^- groups is expected to be higher than Na^+ with the same functional groups.[54] This increasing trend in adhesion energy in $CaCl_2$ solution reached a maximum at 10 mM ionic strength suggesting saturation in the complexation process. For the 1-week membrane sample, the increase in relative difference in adhesion energy was independent of ionic strength and was at the same level as for the 8-h sample in 1 mM NaCl solution. This result suggests that the number of sites susceptible to make complexes with calcium was lower than the foulant deposited at 8 h (i.e., in good accordance with the relative increase of polysaccharides in the foulant) and saturation was already reached at 1 mM NaCl solution. Relative difference in adhesion energy for 2-weeks and 4-weeks membranes was negative (i.e., ca. −60%) at 1 mM NaCl solution and then gradually increased to a positive value with increasing ionic strength. The significant difference between the 8-h sample profile (mainly humic material) and 1-week, or 2-weeks, or 4-weeks sample profiles (mainly nonhumics) suggests foulant layers of different physicochemical properties and are in good agreement with the characterization performed on these samples described in the previous sections. Humic-like substances are more enriched in carboxylic groups than polysaccharides and proteins, and therefore are more prone to make complexes with Ca^{2+} ions than nonhumic substances, which is evidenced by the relative difference in adhesion energies.

3.5. Dynamics of Microbial Communities in SWRO Membrane Biofilms. Differences in organic compounds distribution on the SWRO membranes might have had an impact over bacterial community composition and diversity. To investigate this hypothesis, next generation sequencing of 16S rRNA gene was performed on the RO membranes samples. The overall phyla distribution of 1-week, 2-weeks, and 4-weeks membrane samples revealed that *Proteobacteria* was the dominant phyla corresponding to 80% of total sequences for 1- and 2-weeks membranes and 76% for 4-weeks membrane. The second most represented phylum was *Bacteroidetes* (19% for 1-week, 18% for 2-weeks, and 13% for 4-weeks membranes) (Figure 5A). Noticeably, for the 4-weeks membrane, *Proteobacteria* was almost exclusively represented by *Alphaproteobacteria* class members (60% of sequences) and their distribution was slightly different from that of the other samples. For the 1-week membrane, both *Alphaproteobacteria* and *Gammaproteobacteria* were evenly distributed and each corresponded to 40% of total sequences. For the 2-weeks membrane, *Alphaproteobacteria* representativeness increased up to 51% and the remaining sequences were majorly distributed in *Gammaproteobacteria* (21%) and *Betaproteobacteria* (7%) classes (Figure 5A).

Interestingly, within the *Proteobacteria* phylum, representation of *Alphaproteobacteria* class increased proportionally with increase of operation time. This progressive increase in relative abundance of *Alphaproteobacteria* might be associated with the changes occurring in chemical composition of fouling layer.

The phylogenetic affiliation of the different operational taxonomic units (OTUs), obtained after clustering the sequence data sets revealed that *Antarctobacter*, *Roseobacter* sp, *Rhodobacteraceae*, *Roseovarius nubinhibens*, and *Sulfitobacter* were present in all RO membranes; showing, however, differential concentration profiles. The differences on major species/groups identified on the lab-scale membranes can be observed by the presence of *Methylophaga* (7.6%) and *Pseudidiomarina homiensis* (6.0%), both *Gammaproteobacteria*, and *Sulfitobacter* (3.1%, *Alphaproteobacteria*) in the 1-week membrane sample. However, these species were absent or poorly represented in the 2- and 4-weeks samples (Figure 5B). Interestingly, *Pseudidiomarina homiensis* was identified in a phenanthrene (polycyclic-aromatic hydrocarbon) degrading bacteria screen[55] and its relative high abundance in 1-week membrane coincides with the relatively high PHA concentration in the foulant recovered from this sample. This finding suggests that these species might be associated to an early established biofilm. Conversely, the 4-weeks membrane was majorly dominated by *Antarctobacter sp* (15% of sequences, *Alphaproteobacteria*), which was decreasingly represented in the 2- and 1-week samples, 2.6% and 0.3%, respectively (Figure 5B). Members of *Antarctobacter* genera (*Rhodobacteraceae* family) were associated with hypersaline environments,[56] whereas other *Rhodobacteraceae* affiliated groups, i.e., *Roseobacter* clade and *Roseovarius nubinhibens*, were described as degraders of organic sulfur compounds (dimethylsulfoniopropionate) and generalists of DOC in nutrient-rich environments.[57,58] It is possible that organic sulfur compounds might have accumulated on the RO membrane surface with increasing usage time. *Rhodobacteraceae* family members were also found to be more abundant on other SWRO membranes running for longer periods i.e., one year (Red Sea),[19] 60 and 120 days (Mediterranean Sea),[17] and in another comparative study of differently located SWRO membranes.[1] This indicates that such species should be more adapted to a more mature biofilm where nutrient competition is a rule for the survival of the fittest. These findings corroborate the lower bacterial community diversity found in the 4-weeks old membrane (i.e., Shannon−H index = 4.0 compared to 4.13 and 4.43 for 1-week and 2-weeks membranes, respectively).

3.6. Model of Biofilm Development. Results of direct and indirect characterization of fouling layer suggest that biofilm formation involved multiple steps, including (1) rapid accumulation of humic substances and polysaccharides (predominantly α-linked) on the membrane surface, known as surface conditioning film formation, which helps in the microbial adhesion and may also serve as nutrient for the following initial growth stage, (2) microbial growth, a phase after the settlement/adsorption of cells on membrane surface which leads to the formation of microcolonies, and (3) growth of microcolonies into macrocolonies and release of EPS. Similar biofilm formation models have been proposed and discussed by several researchers.[33,59−61] Studies showing direct and experimental evidence of the steps involved in biofilm development with evolution analyses of both microbial community and chemical substances are, to the best of our knowledge, not available in the literature. Ivnitsky et al.[15] investigated the stages of biofilm development on NF wastewater membrane by imaging techniques (i.e., AFM and CLSM). However, they were unable to observe biofilm development stages similar to

this current study. Recently, changes in the fouling layer of SWRO membrane with operating time, i.e., 2−20 h, have been studied by Monruedee et al.[14] However, this investigation focused only on the major changes in the morphology and elemental composition of the cake layer by AFM and SEM/EDX (scanning electron microscopy/energy dispersive X-ray spectroscopy) techniques. In the field of membrane biofouling, specifically SWRO membranes biofouling, the present work is unique in the sense that it is presenting direct/experimental evidence of stages involved in the biofilm formation on RO membranes, along with detailed observation of evolutionary changes in microbial community and chemical composition. It is worth mentioning that the initial step of biofilm formation, i.e., phenomenon of conditioning film formation, has also been extensively studied by several researchers, but the substrate material and experimental conditions used in those studies were different from that of real RO membrane systems. Different substances have been reported as major and/or primary components involved in the formation of conditioning films, e.g., Baier[10] reported glycoproteins as a main component of conditioning film formed in the process of biofilm development by oral bacteria, humic substances were identified by Loeb and Neihof[47] in the marine water conditioning film formed on platinum plates, proteins were reported by Compère et al.[62] as the first biopolymer absorbed on stainless steel immersed for 2−24 h in natural seawater, and polysaccharides were reported by Garg et al.[63] to be most abundant constituents of organic matter of conditioning film formed on hydrophilic glass panels kept in flowing seawater up to 8 h. Based on detailed foulant characterization data, we identified a specific pattern of temporal predominance of different bacteria and biopolymers in the different stages of biofouling phenomenon of SWRO membrane (Figure 6).

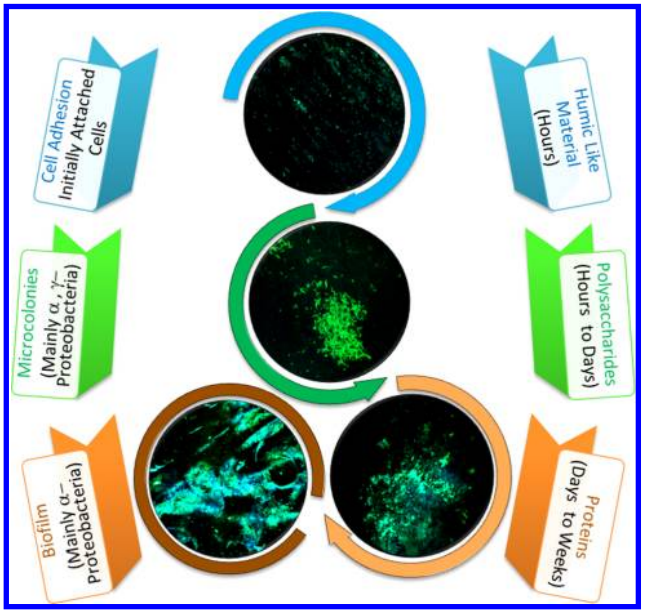

Figure 6. Changes in abundance of organic and microbial components of fouling layer occurring during biofilm formation on SWRO membrane. Identified sequential phases include coating of organics facilitating cell adhesion (*Initial Film Formation*), formation of microcolonies (*Intermediate Phase*), and formation of macrocolonies embedded in released EPS (*Biofilm*).

Increase in representativeness of *Alphaproteobacteria* class with time showed their critical contribution in the biofouling of SWRO membranes. It might be due to higher competitiveness and compatibility features of these bacteria with the chemical environment and hydrodynamic conditions of the SWRO feed channel. Moreover, higher abundance of polycyclic aromatic compound degrading bacteria (i.e., *Pseudidiomarina homiensis*) in 1-week membrane fouling layer, characterized by relatively higher proportion of PHA, is an evidence of the role of the chemistry of the fouling layer in the selection and/or dominance of a particular type of bacteria. Also, continuous increase in both S content and abundance of organic sulfur compound degrading bacteria (i.e., *Roseovarius nubinhibens*) in the fouling layer showed correlation between the profile of microbial community and the chemistry of fouling layer. On the basis of all this information regarding dynamic patterns of SWRO membrane biofouling, further studies aiming toward the development of better strategies against problematic foulants could be undertaken.

■ ASSOCIATED CONTENT

Supporting Information

Additional method details and supplementary figures and tables, including schematic description of the lab-scale unit (Figure S1), model approaching force curve and the corresponding gradient force curve of 8-h sample (Figure S2), feedwater quality analysis data (Figure S3, Table S1, and Table S2) profile of decrease in permeate flux with operating time (Figure S4), ATR-FTIR spectra of virgin and fouled membranes (Figure S5), AFM phase signal on topography picture for virgin and fouled membranes (Figures S6), and pyrochromatograms of foulant materials, humic-like material extracted from Red Sea, and plastic material of tubing used in filtration setup (Figure S7). This material is available free of charge via the Internet at http://pubs.acs.org.

■ AUTHOR INFORMATION

Corresponding Author

*Tel: +966 808 2984; e-mail: jp.croue@kaust.edu.sa.

Notes

The authors declare no competing financial interest.

■ ACKNOWLEDGMENTS

We thank Dr. Wei Xu and Guangchao Wang for help in analyzing samples with confocal laser scanning microscope. Additionally, we thankfully acknowledge the support received from our WDRC lab staff. All the funds for this work were provided by King Abdullah University of Science and Technology (KAUST).

■ REFERENCES

(1) Zhang, M.; Jiang, S.; Tanuwidjaja, D.; Voutchkov, N.; Hoek, E. M. V.; Cai, B. Composition and variability of biofouling organisms in seawater reverse osmosis desalination plants. *Appl. Environ. Microbiol.* **2011**, *77* (13), 4390−4398, DOI: 10.1128/aem.00122-11.

(2) Choi, H.; Park, J.; Tak, T.; Kwon, Y.-N. Surface modification of seawater reverse osmosis (SWRO) membrane using methyl methacrylate-hydroxy poly(oxyethylene) methacrylate (MMA-HPOEM) comb-polymer and its performance. *Desalination* **2012**, *291* (0), 1−7, DOI: 10.1016/j.desal.2012.01.018.

(3) Drioli, E.; Macedonio, F. Membrane engineering for water engineering. *Ind. Eng. Chem. Res.* **2012**, *51* (30), 10051−10056, DOI: 10.1021/ie2028188.

(4) Valavala, R.; Sohn, J.; Han, J.; Her, N.; Yoon, Y. Pretreatment in reverse osmosis seawater desalination: A short review. *Environ. Eng. Res.* **2011**, *16* (4), 205−212, http://dx.doi.org/10.4491/eer.2011.16.4.205.

(5) Tu, K. L.; Chivas, A. R.; Nghiem, L. D. Effects of membrane fouling and scaling on boron rejection by nanofiltration and reverse osmosis membranes. *Desalination* **2011**, *279* (1−3), 269−277, DOI: 10.1016/j.desal.2011.06.019.

(6) Kang, G.-d.; Liu, Z.-n.; Yu, H.-j.; Cao, Y.-m. Enhancing antifouling property of commercial polyamide reverse osmosis membrane by surface coating using a brush-like polymer containing poly(ethylene glycol) chains. *Desalin. Water Treat.* **2012**, *37* (1−3), 139−145, DOI: 10.1080/19443994.2012.661265.

(7) Tang, C. Y.; Kwon, Y.-N.; Leckie, J. O. The role of foulant-foulant electrostatic interaction on limiting flux for RO and NF membranes during humic acid fouling–Theoretical basis, experimental evidence, and AFM interaction force measurement. *J. Membr. Sci.* **2009**, *326* (2), 526−532.

(8) Sadr Ghayeni, S. B.; Beatson, P. J.; Schneider, R. P.; Fane, A. G. Adhesion of waste water bacteria to reverse osmosis membranes. *J. Membr. Sci.* **1998**, *138* (1), 29−42, DOI: 10.1016/s0376-7388(97)00196-8.

(9) Schneider, R. P.; Marshall, K. C. Retention of the Gramnegative marine bacterium SW8 on surfaces — Effects of microbial physiology, substratum nature and conditioning films. *Colloid Surf., B* **1994**, *2* (4), 387−396, DOI: 10.1016/0927-7765(94)80002-2.

(10) Baier, R. E. Conditioning surfaces to suit the biomedical environment: Recent progress. *J. Biomech. Eng.* **1982**, *104* (4), 257−271.

(11) Flemming, H.-C. Reverse osmosis membrane biofouling. *Exp. Therm Fluid Sci.* **1997**, *14* (4), 382−391.

(12) Melo, L. F.; Bott, T. R.; Bernardo, C. A. *Fouling Science and Technology*; Kluwer Academic Publishers: Norwell, MA, 1988.

(13) Flemming, H. C.; Schaule, G. Biofouling on membranes - A microbiological approach. *Desalination* **1988**, *70* (1−3), 95−119, DOI: 10.1016/0011-9164(88)85047-1.

(14) Monruedee, M.; Sarp, S.; Lee, Y. G.; Kim, J. H. Time-series image analysis for investigating SWRO fouling mechanism. *Desalin. Water Treat.* **2012**, *43* (1−3), 212−220, DOI: 10.1080/19443994.2012.672174.

(15) Ivnitsky, H.; Katz, I.; Minz, D.; Volvovic, G.; Shimoni, E.; Kesselman, E.; Semiat, R.; Dosoretz, C. G. Bacterial community composition and structure of biofilms developing on nanofiltration membranes applied to wastewater treatment. *Water Res.* **2007**, *41* (17), 3924−3935, DOI: 10.1016/j.watres.2007.05.021.

(16) Khedr, M. G. Membrane fouling problems in reverse osmosis desalination applications. *Desalin. Water Reuse* **2002**, *10*, 3−10.

(17) Manes, C. L. d. O.; West, N.; Rapenne, S.; Lebaron, P. Dynamic bacterial communities on reverse-osmosis membranes in a full-scale desalination plant. *Biofouling* **2011**, *27* (1), 47−58, DOI: 10.1080/08927014.2010.536980.

(18) Hörsch, P.; Gorenflo, A.; Fuder, C.; Deleage, A.; Frimmel, F. H. Biofouling of ultra- and nanofiltration membranes fordrinking water treatment characterized by fluorescence in situ hybridization (FISH). *Desalination* **2005**, *172* (1), 41−52, DOI: 10.1016/j.desal.2004.05.009.

(19) Khan, M. T.; Manes, C.-L. d. O.; Aubry, C.; Croué, J.-P. Source water quality shaping different fouling scenarios in a full-scale desalination plant at the Red Sea. *Water Res.* **2013**, *47* (2), 558−568, http://dx.doi.org/10.1016/j.watres.2012.10.017.

(20) ASTM Standard D4189-07. *Standard Test Method for Silt Density Index (SDI) of Water*; 2007; doi 10.1520/D4189-07, www.astm.org.

(21) Reasoner, D. J.; Geldreich, E. E. A new medium for the enumeration and subculture of bacteria from potable water. *Appl. Environ. Microbiol.* **1985**, *49* (1), 1−7.

(22) Nocker, A.; Richter-Heitmann, T.; Montijn, R.; Schuren, F.; Kort, R. Discrimination between live and dead cells in bacterial communities from environmental water samples analyzed by 454 pyrosequencing. *Int. Microbiol.* **2010**, *13* (2), 59−65.

(23) McElroy, W. D. The energy source for bioluminescence in an isolated system. *Proc. Natl. Acad. Sci., U. S. A.* **1947**, *33* (11), 342−345.

(24) Amy, G. L.; Salinas Rodriguez, S. G.; Kennedy, M. D.; Schippers, J. C.; Rapenne, S.; Remize, P.-J.; Barbe, C.; Manes, C.-L. d. O.; West, N. J.; Lebaron, P.; Van der Kooij, D.; Veenendaal, H.; Schaule, G.; Petrowski, K.; Huber, S.; Sim, L. N.; Ye, Y.; Chen, V.; Fane, A. G. Water quality assessment tools. In *Membrane-Based Desalination: An Integrated Approach (MEDINA)*; Drioli, E.,Criscuoli, A., Macedonio, F., Eds.; IWA Publishing: London, UK, 2011; pp 3−31.

(25) Leenheer Jerry, A.; Croué, J.-P.; Benjamin, M.; Korshin Gregory, V.; Hwang Cordelia, J.; Bruchet, A.; Aiken George, R. Comprehensive isolation of natural organic matter from water for spectral characterizations and reactivity testing. In *Natural Organic Matter and Disinfection By-Products*; Barrett, S. E., Krasner, S. W. ,Amy, G. L., Eds.; American Chemical Society: Washington, DC, 2000; pp 68−83.

(26) Chen, M.-Y.; Lee, D.-J.; Yang, Z.; Peng, X. F.; Lai, J. Y. Fluorecent staining for study of extracellular polymeric substances in membrane biofouling layers. *Environ. Sci. Technol.* **2006**, *40* (21), 6642−6646, DOI: 10.1021/es0612955.

(27) Chen, M.-Y.; Lee, D.; Tay, J. Distribution of extracellular polymeric substances in aerobic granules. *Appl. Microbiol. Biotechnol.* **2007**, *73* (6), 1463−1469, DOI: 10.1007/s00253-006-0617-x.

(28) Hutter, J. L.; Bechhoefer, J. Calibration of atomic-force microscope tips. *Rev. Sci. Instrum.* **1993**, *64* (7), 1868 DOI: 10.1063/1.1143970.

(29) Li, X.; Logan, B. E. Analysis of bacterial adhesion using a gradient force analysis method and colloid probe atomic force microscopy. *Langmuir* **2004**, *20* (20), 8817−8822, DOI: 10.1021/la0488203.

(30) Gordesli, F. P.; Abu-Lail, N. I. Impact of ionic strength of growth on the physiochemical properties, structure, and adhesion of *Listeria monocytogenes* polyelectrolyte brushes to a silicon nitride surface in water. *J. Colloid Interface Sci.* **2012**, *388* (1), 257−267, http://dx.doi.org/10.1016/j.jcis.2012.08.048.

(31) Qian, P. Y.; Wang, Y.; Lee, O. O.; Lau, S. C.; Yang, J.; Lafi, F. F.; Al-Suwailem, A.; Wong, T. Y. Vertical stratification of microbial communities in the Red Sea revealed by 16S rDNA pyrosequencing. *ISME J.* **2011**, *5* (3), 568−568, DOI: 10.1038/ismej.2010.159.

(32) Han, Y.; Lin, Q. Effects of inorganics on RO membrane initial biofouling formation. In *3rd International Conference on Bioinformatics and Biomedical Engineering (ICBBE 2009)*, 2009, Beijing, China; pp 1−4.

(33) Flemming, H.-C.; Wingender, J. The biofilm matrix. *Nat. Rev. Microbiol.* **2010**, *8* (9), 623−633.

(34) Hong, S.; Elimelech, M. Chemical and physical aspects of natural organic matter (NOM) fouling of nanofiltration membranes. *J. Membr. Sci.* **1997**, *132* (2), 159−181.

(35) Leenheer, J. A. Systematic approaches to comprehensive analyses of natural organic matter. *Ann. Environ. Sci.* **2009**, *3*, 1−130.

(36) Barth, A.; Zscherp, C. What vibrations tell about proteins. *Q. Rev. Biophys.* **2002**, *35* (04), 369−430, DOI: 10.1017/S0033583502003815.

(37) Naumann, D.; Schultz, C.; Helm, D. What can infrared spectroscopy tell us about the structure and composition of intact bacterial cells? In *Infrared Spectroscopy of Biomolecules*; Mantsch, H. H., Chapman, D., Eds.; John Wiley & Sons: New York, 1996; pp 279−310.

(38) Coates, J. Interpretation of infrared spectra, a practical approach. In *Encyclopedia of Analytical Chemistry*; Meyers, R. A., Ed.; John Wiley & Sons, Ltd: Chichester, U.K., 2000; pp 10815−10837.

(39) Handke, M. Vibrational spectra, force constants, and Si-O bond character in calcium silicate crystal structure. *Appl. Spectrosc.* **1986**, *40* (6), 871−877.

(40) Bruchet, A.; Rousseau, C.; Mallevialle, J. Pyrolysis-GC-MS for investigating high-molecular-weight THM precursors and other refractory organics. *J. Am. Water Works Assoc.* **1990**, *82* (9), 66−74.

(41) Leenheer, J. A.; Croué, J.-P. Peer reviewed: Characterizing aquatic dissolved organic matter. *Environ. Sci. Technol.* **2003**, *37* (1), 18A−26A, DOI: 10.1021/es032333c.
(42) Bhaskar, P. V.; Bhosle, N. B. Microbial extracellular polymeric substances in marine biogeochemical processes. *Curr. Sci.* **2005**, *88* (1), 45−53.
(43) Azam, F.; Simon, M. Protein content and protein synthesis rates of planktonic marine bacteria. *Mar. Ecol.: Prog. Ser.* **1989**, *51*, 201−213.
(44) Gillam, A. H.; Wilson, M. A. Pyrolysis-GC-MS and NMR studies of dissolved seawater humic substances and isolates of a marine diatom. *Org. Geochem.* **1985**, *8* (1), 15−25, DOI: 10.1016/0146-6380(85)90046-4.
(45) Wilson, M. A.; Philp, R. P.; Gillam, A. H.; Gilbert, T. D.; Tate, K. R. Comparison of the structures of humic substances from aquatic and terrestrial sources by pyrolysis gas chromatography-mass spectrometry. *Geochim. Cosmochim. Acta* **1983**, *47* (3), 497−502, DOI: 10.1016/0016-7037(83)90272-7.
(46) Kusch, P. Pyrolysis-gas chromatography/mass spectrometry of polymeric materials In *Advanced Gas Chromatography - Progress in Agricultural, Biomedical and Industrial Applications*; InTech: Rijeka, Croatia, 2012; pp 333−362. Available from: http://cdn.intechopen.com/pdfs/32828/InTech-Pyrolysis_gas_chromatography_mass_spectrometry_of_polymeric_materials.pdf.
(47) Loeb, G. I.; Neihof, R. A. Marine conditioning films. In *Applied Chemistry at Protein Interfaces*; Baier, R. E., Ed.; American Chemical Society: Washington, DC, 1975; pp 319−335.
(48) Derjaguin, B. Untersuchungen über die Reibung und Adhäsion, IV. *Colloid Polym. Sci.* **1934**, *69* (2), 155−164, DOI: 10.1007/bf01433225.
(49) Verwey, E. J. W.; Overbeek, J. T. G. *Theory of the Stability of Lyophobic Colloids*; Elsevier: Amsterdam, 1948.
(50) Dorobantu, L. S.; Bhattacharjee, S.; Foght, J. M.; Gray, M. R. Analysis of force interactions between AFM tips and hydrophobic bacteria using DLVO theory. *Langmuir* **2009**, *25* (12), 6968−6976, DOI: 10.1021/la9001237.
(51) Aubry, C.; Gutierrez, L.; Croue, J. P. Coating of AFM probes with aquatic humic and non-humic NOM to study their adhesion properties. *Water Res.* **2013**, *47*, 3109−3119, http://dx.doi.org/10.1016/j.watres.2013.03.023.
(52) Xu, L.-C.; Logan, B. E. Interaction forces between colloids and protein-coated surfaces measured using an atomic force microscope. *Environ. Sci. Technol.* **2005**, *39* (10), 3592−3600, DOI: 10.1021/es048377i.
(53) Kalinichev, A. G.; Kirkpatrick, R. J. Molecular dynamics simulation of cationic complexation with natural organic matter. *Eur. J. Soil Sci.* **2007**, *58* (4), 909−917, DOI: 10.1111/j.1365-2389.2007.00929.x.
(54) Stumm, W. Chemical interaction in particle separation. *Environ. Sci. Technol.* **1977**, *11* (12), 1066−1070, DOI: 10.1021/es60135a010.
(55) Jean, W. D.; Leu, T.-Y.; Lee, C.-Y.; Chu, T.-J.; Lin, S. Y.; Shieh, W. Y. *Pseudidiomarina marina* sp. nov. and *Pseudidiomarina tainanensis* sp. nov. and reclassification of *Idiomarina homiensis* and *Idiomarina salinarum* as *Pseudidiomarina homiensis* comb. nov. and *Pseudidiomarina salinarum* comb. nov., respectively. *Int. J. Syst. Evol. Microbiol.* **2009**, *59* (1), 53−59, DOI: 10.1099/ijs.0.001180-0.
(56) Labrenz, M.; Collins, M. D.; Lawson, P. A.; Tindall, B. J.; Braker, G.; Hirsch, P. *Antarctobacter heliothermus* gen. nov., SP. now, a budding bacterium from hypersaline and heliothermal Ekho Lake. *Int. J. Syst. Bacteriol.* **1998**, *48*, 1363−1372.
(57) Malmstrom, R. R.; Kiene, R. P.; Cottrell, M. T.; Kirchman, D. L. Contribution of SAR11 bacteria to dissolved dimethylsulfoniopropionate and amino acid uptake in the north Atlantic ocean. *Appl. Environ. Microbiol.* **2004**, *70* (7), 4129−4135, DOI: 10.1128/aem.70.7.4129-4135.2004.
(58) Poretsky, R. S.; Sun, S.; Mou, X.; Moran, M. A. Transporter genes expressed by coastal bacterioplankton in response to dissolved organic carbon. *Environ. Microbiol.* **2010**, *12* (3), 616−627, DOI: 10.1111/j.1462-2920.2009.02102.x.
(59) Flemming, H.-C. Microbial biofouling: Unsolved problems, insufficient approaches, and possible solutions. In *Biofilm Highlights*; Flemming, H.-C., Wingender, J., Szewzyk, U., Eds.; Springer: Berlin-Heidelberg, 2011; pp 81−109.
(60) Guo, W.; Ngo, H.-H.; Li, J. A mini-review on membrane fouling. *Bioresour. Technol.* **2012**, *122* (0), 27−34, DOI: 10.1016/j.biortech.2012.04.089.
(61) Bar-Zeev, E.; Berman-Frank, I.; Girshevitz, O.; Berman, T. Revised paradigm of aquatic biofilm formation facilitated by microgel transparent exopolymer particles. *Proc. Natl. Acad. Sci., U. S. A.* **2012**, *109* (23), 9119−9124, DOI: 10.1073/pnas.1203708109.
(62) Compère, C.; Bellon-Fontaine, M. N.; Bertrand, P.; Costa, D.; Marcus, P.; Poleunis, C.; Pradier, C. M.; Rondot, B.; Walls, M. G. Kinetics of conditioning layer formation on stainless steel immersed in seawater. *Biofouling* **2001**, *17* (2), 129−145, DOI: 10.1080/08927010109378472.
(63) Garg, A.; Jain, A.; Bhosle, N. B. Chemical characterization of a marine conditioning film. *Int. Biodeterior. Biodegrad.* **2009**, *63* (1), 7−11, DOI: 10.1016/j.ibiod.2008.05.004.